

Applications of survival functions to continuous semi-Markov processes for measuring reliability of power transformers

Yifei WANG¹, Mohammad SHAHIDEHPOUR², Chuangxin GUO³



Abstract The reliability of power transformers is subject to service age and health condition. This paper proposes a practical model for the evaluation of two reliability indices: survival function (SF) and mean residual life (MRL). In the proposed model, the periodical modeling of power transformers are considered for collecting the information on health conditions. The corresponding health condition is assumed to follow a continuous semi-Markov process for representing a state transition. The proportional hazard model (PHM) is introduced to incorporate service age and health condition into hazard rate. In addition, the proposed model derives the analytical formulas for and offers the analytical evaluation of SF and MRL. SF and MRL are calculated for new components and old components, respectively. In both cases, the proposed model offers rational results which are compared with those obtained from comparative models. The results obtained by the contrast of the proposed analytical method and the Monte Carlo method. The impact of different

model parameters and the coefficient of variation (CV) on reliability indices are discussed in the case studies.

Keywords Power system reliability, Transformers, Proportional hazard model, Survival function, Mean residual life, Semi-Markov process

1 Introduction

The equipment reliability is subject to degradation and influencing factors which are referred to as covariates. The evaluation of system reliability has gained additional interests for quantifying the risk of degradation and failure, predicting the performance, making economic decisions in large-scale energy, transportation, and telecommunication infrastructures. Considering the example of a 750 kV electric power transformer with a typical capital cost of \$ 2 million [1], the failure of such equipment could cause extensive outages and blackouts and raise customer interruption costs. It is therefore imperative to monitor the equipment health condition and evaluate its reliability to avoid catastrophic circumstances.

We consider two reliability indices: survival function (SF) and mean residual life (MRL). SF is the probability that the equipment will survive beyond a specified time. MRL renders an overall estimate and summarizes the residual life distribution of the equipment. Several failure rate models are considered for calculating the two reliability indices. However, a constant failure rate model is often used in reliability analyses which can pose erroneous results for the calculation of reliability indices [2–4].

The failure rate calculation should take both service age and covariates into consideration. The proportional hazard model (PHM) was introduced by Cox in 1972 to shape the

CrossCheck date: 10 July 2017

Received: 7 January 2016 / Accepted: 10 July 2017 / Published online: 22 September 2017

© The Author(s) 2017. This article is an open access publication

✉ Mohammad SHAHIDEHPOUR
ms@iit.edu

Yifei WANG
wangyifei@gdut.edu.cn

Chuangxin GUO
guochuangxin@zju.edu.cn

¹ School of Automation, Guangdong University of Technology, Guangzhou 510006, China

² Galvin Center for Electricity Innovation, Illinois Institute of Technology, Chicago, IL 60616, USA

³ College of Electrical Engineering, Zhejiang University, Hangzhou 310058, China



hazard rate used in engineering and medicine [5, 6]. In PHM, the hazard rate consists of baseline and link functions. The baseline function offers the basis for hazard rate and the link function quantifies the covariate effect. Sample covariates such as those pertaining to the lifecycle data [7], operation mode [8], vibration [9] and dissolved gas [10], which could be time-dependent, are considered according to the actual system situations. PHM offers advantages when applied to explanatory techniques [11]. Accordingly, the model adopts the information on dissolved gas analysis (DGA) as covariate which affects the failure rates of power transformers.

The MRL and conditional/unconditional SFs are calculated in [12] by a discrete Markov process and PHM for obtaining the additional insight on interactions between time-varying failure rates and reliability indices. Makis and Jardine [13] utilize a full parametric PHM and a time-homogeneous Markov chain to describe failure rates. Accordingly, the optimal expected average cost and replacement time are obtained. Reference [14] evaluates the equipment reliability with imperfect observations. The observations are collected periodically. The failure rate is modeled based on PHM which takes both the age and the health condition into consideration. The same model is adopted to identify the optimal inspection period and the replacement policy [15]. The parameter estimation problem is studied in [16]. A control-limit policy and parameter estimation are proposed in [17] where an optimal replacement policy is obtained to minimize the average replacement costs per unit time. The above models are based on the assumption that the condition information of covariates is inspected at discrete points and every state transition happens only at the end of inspection interval, exactly before the next inspection instant, to make the calculation tractable within every interval. These models are called discrete monitoring and discrete transition (DMDT) models in this paper.

In fact, the state transition can happen at any time and this assumption may not conform to the reality. Reference [18] evaluates the SF policy by applying PHM and the presumption that the state transition is continuous. Reference [19] also assumes the condition monitoring is continuous if the inspection interval is small. These models are called

continuous monitoring and continuous transition (CMCT) models in this paper. However, the condition monitoring may not be continuous in practice and the assumption would not be in line with the actual operation.

In practice, the online condition monitoring of power transformers, such as dissolved gas analysis, is discrete (periodical) while the state transition could happen at any time [20, 21]. In this paper we propose the discrete monitoring and continuous transition (DMCT) models for our analyses. The parameter estimation is found in [22] which is not addressed in this paper. The main contributions of this paper offered by our model are summarized below:

- 1) The proposed model is based on more practical assumptions in which the condition is discretely inspected but the state transition is continuous.
- 2) Service age and DGA information are introduced to customize the failure rate by applying PHM. The state transition of DGA is described by a semi-Markov process.
- 3) Analytical formulas are derived to evaluate SF and MRL using the given situations. The effectiveness of the proposed formulas is shown in our numerical studies.

2 Model description

2.1 Determine health condition with DGA information

All power transformers generate gases to some extent when they are operating normally. However, the incipient fault or degradation, such as overheating, partial discharge and arcing faults, will lead to the abnormality of gas-generating. A four-level criterion has been developed to classify health condition of transformers [23] according to the gases concentration. The gases include H_2 , CH_4 , C_2H_4 , C_2H_6 , CO , and CO_2 . The total gas of H_2 , CH_4 , C_2H_4 , C_2H_6 , CO is known as total dissolved combustible gases concentration (TDGC). Table 1 shows the classification of gas concentration conditions. Condition (1) is the best condition, and the condition gets worse with the number

Table 1 Dissolved gas concentrations for condition classification based on IEEE C57.104

Condition	Dissolved gas concentration ($\mu\text{L/L}$)							
	H_2	CH_4	C_2H_2	C_2H_4	C_2H_6	CO	CO_2	TDGC
1	<100	<120	<35	<50	<65	<350	<2500	<720
2	100–700	121–400	36–50	51–100	66–100	351–570	2500–4000	721–1920
3	700–1800	401–1000	51–80	101–200	101–150	571–1400	4001–10000	1921–4630
4	>1800	>1000	>80	>200	>150	>1400	>10000	>4630

increases. The power transformer is regarded as being in the worse condition irrespective of the type of dissolved gas that is in the worse condition. In other words, the condition of power transformer depends on the worst condition of all the dissolved gases.

2.2 Failure rate model based on DGA information

The failure rate of power transformer is modelled by PHM and semi-Markov process. The failure rate is expressed as:

$$h(s, Z(s)) = h_0(s)\psi(Z(s)) = \frac{\beta s^{\beta-1}}{\alpha^\beta} e^{\gamma Z(s)} \tag{1}$$

where $h_0(s)$ is the baseline function to describe basic hazard rate; $\psi(Z(s))$ is the link function to quantify the effect of covariates. The covariate $Z(s)$ represents the condition of dissolved gas concentrations at time s . The degradation process is irreversible, which is the most common case that the degradation state cannot improve by itself. Without loss of generality, the gas condition $Z(s)$ is assumed to fall into finite state space $\{1, 2, \dots, n\}$ where the condition deteriorates as the state number increases. The analytical formulas are also derived with n conditions. The state n is the worst and absorbing state. Upon a failure or scheduled maintenance, the component is maintained and restored to state 1 and the process is renewed. The model is shown in Fig. 1 which is described as follows:

- 1) $T_i, X_i, i = 1, 2, \dots, n$, denote the i th state transition moment and the sojourn time of state i , respectively.
- 2) t_0 and t are the current time and future time point, respectively.
- 3) The transition of health condition is assumed to follow a semi-Markov process. The transition is irreversible and increases by one whenever a transition occurs. That is, a pure birth process is considered.

The Markov process is memoryless and Markov models can lead to serious errors on certain conditions. However, the health condition transition of a power transformer is affected by the operation history which is not a memoryless process. In our study, a semi-Markov process is introduced

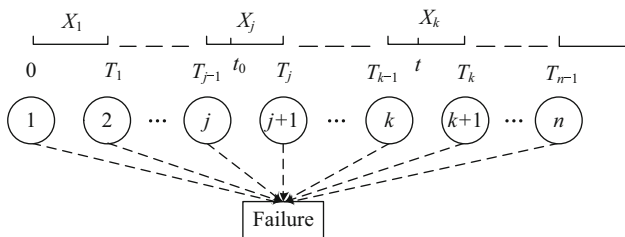


Fig. 1 Degradation and failure process

to describe the memorial degradation process of power transformers and evaluate reliability indices. In our case studies, the results of the contrast of Markov and semi-Markov processes and some reasonable conclusions have been drawn. Other stochastic processes could also be also introduced to model the condition transition indeed. Based on our proposed model, we plan on performing more work in the future to compare the performance of different stochastic process when evaluating the reliability of power transformers.

Let Z_i denote the degradation state between T_{i-1} and T_i . In a pure birth process $Z_i = i$. Since the state n is an absorbing state, we define $X_n = \infty$ and $T_n = \infty$. Clearly $X_i = T_i - T_{i-1}$ and its distribution is denoted as:

$$G(x_i) = P(T_i - T_{i-1} \leq x_i | Z_i = i, Z_{i+1} = i + 1) \tag{2}$$

where x_i is the independent variable in the distribution function of X_i . The state sojourn time X_1, X_2, \dots, X_n are conditional independent in a semi-Markov process. That is, the Markovian property is satisfied at the transition point rather than the entire process.

The joint probability density function (PDF) of X_1, X_2, \dots, X_n is represented as g_x which equals to $g(x_1, x_2, \dots, x_{n-1}) = g_1 g_2 \dots g_{n-1}$, where $g_i = g(x_i)$ is the probability density function of x_i .

It should be noted that:

$$T_k = \sum_{i=1}^k X_i = X_1 + X_2 + \dots + X_k \tag{3}$$

and

$$Z(t) = k \Leftrightarrow T_{k-1} \leq t < T_k \tag{4}$$

where $Z(t)$ is the gas concentration state at time t . The conditional survival function $R(t|t_0)$ is given by:

$$P(T \geq t | T > t_0, Z(s), 0 \leq s \leq t_0) = \exp\left(-\int_{t_0}^t h(s, Z(s)) ds\right) \tag{5}$$

where T is the failure time. Given t_0 and $Z(t_0) = j$, the component or the system may stay at an arbitrary state from j to n at any future time t . For $Z(t_0) = j, Z(t) = k, 1 \leq j \leq k \leq n$, we have:

$$R_{jk}(t|t_0) = P(T > t | T > t_0, Z(t_0) = j, Z(t) = k) = \exp\left(-\int_{t_0}^{T_j} h(s, Z_j) ds - \int_{T_j}^{T_{j+1}} h(s, Z_{j+1}) ds - \dots - \int_{T_{k-1}}^t h(s, Z_k) ds\right) \tag{6}$$

If we view $(X_1, X_2, \dots, X_{n-1})$ as a $(n-1)$ dimensional space, (6) would be satisfied only in the sub-region D_{jk} .



$$D_{jk} = \left\{ (X_1, X_2, \dots, X_{n-1}) \left| \begin{array}{l} x_1 + \dots + x_{j-1} \leq t_0 \\ x_1 + \dots + x_j > t_0 \\ x_1 + \dots + x_{k-1} \leq t \\ x_1 + \dots + x_k > t \\ x_i \geq 0, 1 \leq i \leq n-1 \end{array} \right. \right\} \quad (7)$$

In this paper, x_i is assumed to be larger than zero. For instance, $D_{12} = \{(X_1, X_2, \dots, X_n) | x_1 > t_0, x_1 \leq t < x_1 + x_2\}$, when $j = 1, k = 2$ in (7), which means the component is in state 1 at t_0 and state 2 at t . Also, in the area D_{12} , $R_{12}(t|t_0) = \exp(-\int_{t_0}^t h(s, Z_1)ds - \int_t^t h(s, Z_2)ds)$. Thus, when the state at any future time t varies from 1 to n , $R(t|t_0)$ can be viewed as a piecewise function in the n dimensional space $\{R(t|t_0), X_1, \dots, X_{n-1}\}$. Accordingly, $R_{jk}(t|t_0)$ represents $R(t|t_0)$ in the sub-region D_{jk} . The boundary of each sub-region is decided by t_0 and t , and the corresponding degradation states $Z(t_0)$ and $Z(t)$.

Generally, MRL is calculated by $M(t_0) = \int_{t_0}^{\infty} R(t|t_0)dt$. Since $R(t|t_0)$ is a piecewise function from t_0 to infinity, the conditional MRL, given t_0 and $Z(t_0) = j$, can be expressed as:

$$\begin{aligned} m_j(t_0) &= \int_{t_0}^{\infty} R(t|t_0)dt = \int_{t_0}^{T_j} R_{jj}(t|t_0)dt \\ &+ \int_{T_j}^{T_{j+1}} R_{j,j+1}(t|t_0)dt + \dots + \int_{T_{n-1}}^{\infty} R_{jn}(t|t_0)dt \\ &= \sum_{i=j}^n M_{jk}(t_0) = M_{jj}(t_0) + M_{j,j+1}(t_0) + \dots + M_{jn}(t_0) \end{aligned} \quad (8)$$

where $M_{ji}(t_0) = \int_{T_{j-1}}^{T_i} R_{ji}(t|t_0)dt$ for $j < i \leq n$.

With (5), (6) and (8) in place, there is still one barrier in evaluating SF and MRL, effectively, where the explicit analytical expressions are needed.

3 Evaluating SF and MRL

The DGA is inspected at discrete points, and the inspection instants are equally spaced. Figure 2 shows the inspection points, state transition points and time points, where Δ_l means the l th inspection point, S1 and S2 represent two different situations, respectively.

The formulas are presented in two situations: t_0 (S1) is exactly the inspection point and t_0 (S2) is between the inspection points. The t_0 point exhibits a big influence on the expression and the shape of SF and MRL. In fact,

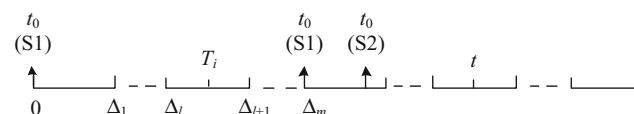


Fig. 2 Inspection points, transition points and time points

whether t_0 is the inspection point has a practical significance. The t_0 as the exact inspection point corresponds to the situation where the DGA condition information has just been collected from an on-line or off-line test, while the t_0 located between two successive inspection points corresponds to a situation where the condition inspection by either an on-line or off-line test has been done before and the next inspection point has not been reached. Both S1 and S2 situations could occur in practice.

Note that SF and MRL are the functions of random variables X_1, X_2, \dots, X_{n-1} , which are multiple integral in the variable space. The known conditions constitute the composite constraint surface of the integral region. In this section, the multiple integral is transformed to the repeated integral to derive the formulas of SF and MRL.

3.1 Survival function

The survival function is a piecewise function associated with random variables which is calculated by the conception of expectation.

1) A new component

For a new component, we have $t_0 = 0, Z(t_0) = 1$. According to the Law of Total Probability, $R(t)$ can be expressed as:

$$\begin{aligned} R(t) &= \sum_{k=1}^n P(T > t, Z(t) = k | Z(t_0) = 1) \\ &= \sum_{k=1}^n \int_{D_{1k}} R_{1k}(t)g(x_1, \dots, x_k)dx_1 \dots dx_k \\ &= r_{11} + r_{12} + \dots + r_{1n} \end{aligned} \quad (9)$$

where $r_{1k} = \int_{D_{1k}} R_{1k}(t)g(x_1, \dots, x_{n-1})dx_k \dots dx_1, k = 1, 2, \dots, n - 1$ can be calculated as follows:

$$r_{1k} = \begin{cases} \int_0^t \int_0^{t-x_1} \dots \int_0^{t-T_{k-2}} \int_{t-T_{k-1}}^{\infty} R_{1k}(t)g_x dx_k \dots dx_2 dx_1 & k = 1, 2, \dots, n-1 \\ \int_0^t \int_0^{t-x_1} \dots \int_0^{t-T_{n-2}} \int_0^{t-T_{n-1}} R_{1n}(t)g_x dx_{n-1} \dots dx_1 & k = n \end{cases} \quad (10)$$

The proof of (10) is presented in Appendix A.

2) An old component

An old component has survived and suffered from degradation by the time t_0 . Assuming the last inspection instant is Δ_m and $Z(\Delta_m) = j$, we have $T_j > \Delta_m$. In fact, state transition points are renewal points and have Markovian property [3], thus the state transition after T_{j-1} has nothing to do with the history before and can happen at any time.

The calculation of survival function falls into the two cases which are designated as old1 and old2.

Situation S1: t_0 is exactly the inspection instant Δ_m . In this case, the known conditions are given: ① $T > t_0$; ② $Z(t_0) = j$; ③ X_1, X_2, \dots, X_{j-1} . According to the Law of Total Probability, $R(t|t_0)$ is equal to:

$$R(t|t_0) = \sum_{k=j}^n P(T > t, Z(t) = k | T > t_0, Z(t_0) = j) = \sum_{k=j}^n \int_{D_{jk}} R_{jk}(t|t_0) g_{x|x_j} dx_j \dots dx_{n-1} \tag{11}$$

Let r_{jk}^{old1} denote $\int_{D_{jk}} R_{jk}(t|t_0) g_{x|x_j} dx_j \dots dx_{n-1}$ and r_{jk}^{old1} can be calculated by (12). The proof is shown in [Appendix B](#).

$$r_{jk}^{old1} = \begin{cases} \int_{t_0-T_{j-1}}^{t-T_{j-1}} \int_0^{t-T_{j-1}-x_j} \dots \int_0^{t-x_1-\dots-x_{k-2}} \int_{t-x_1-\dots-x_{k-1}}^{\infty} R_{jk}(t|t_0) g_{x|x_j} dx_k \dots dx_j & j \leq k < n \\ \int_{t_0-T_{j-1}}^{t-T_{j-1}} \int_0^{t-T_{j-1}-x_j} \dots \int_0^{t-x_1-\dots-x_{k-2}} \int_0^{t-x_1-\dots-x_{n-1}} R_{jn}(t|t_0) g_{x|x_j} dx_{n-1}, \dots dx_j & k = n \end{cases} \tag{12}$$

Situation S2: t_0 is between two successive inspection instants Δ_m and Δ_{m+1} .

In this case, $Z(t_0)$ can be arbitrarily selected from $Z(\Delta_m)$ to n since t_0 is not an inspection point. The known conditions are given: ① $T > t_0$; ② $Z(\Delta_m) = j$; ③ X_1, X_2, \dots, X_{j-1} . $R(t|t_0)$ is denoted by:

$$R(t|t_0) = P(T > t | T > t_0, Z(\Delta_m) = j) = \sum_{i=j}^n \sum_{k=i}^n P(T > t, Z(t) = k, Z(t_0) = i | T > t_0, Z(\Delta_m) = j) = \sum_{i=j}^n \sum_{k=i}^n \int_{D_{ik}} R_{ik}(t|t_0) g_{x|x_j} dx_j \dots dx_{n-1} \tag{13}$$

Let $r_{j,ik}^{old2}$ be $\int_{D_{ik}} R_{ik}(t|t_0) g_{x|x_j} dx_j \dots dx_{n-1}$ which represents the survival probability in the sub-region $Z(\Delta_m) = j$, $Z(t_0) = i$ and $Z(t) = k$. $r_{j,ik}^{old2}$ can be evaluated by (14). The proof is shown in [Appendix C](#).

$$r_{j,ik}^{old2} = \begin{cases} \int_{\Delta_m-T_{j-1}}^{t_0-T_{j-1}} \int_0^{t_0-T_{j-1}-x_j} \dots \int_{t_0-x_1-\dots-x_{i-1}}^{t-x_1-\dots-x_{i-1}} \dots \int_0^{t-x_1-\dots-x_{k-2}} \int_{t-x_1-\dots-x_{k-1}}^{\infty} R_{jk}(t|t_0) g_{x|x_j} dx_j \dots dx_k & i \leq k < n \\ \int_{\Delta_m-T_{j-1}}^{t_0-T_{j-1}} \int_0^{t_0-T_{j-1}-x_j} \dots \int_{t_0-x_1-\dots-x_{i-1}}^{t-x_1-\dots-x_{i-1}} \dots \int_0^{t-x_1-\dots-x_{n-2}} \int_0^{t-x_1-\dots-x_{n-1}} R_{jk}(t|t_0) g_{x|x_j} dx_{n-1} \dots dx_j & k = n \end{cases} \tag{14}$$

3.2 Mean residual life

We evaluate MRL for a new component and an old component, respectively. For an old component, MRL is also calculated in two cases according to whether t_0 is the inspection instant.

1) A new component

For a new component, $t_0 = 0$, $Z(t_0) = 1$, according to (8) MRL can be expressed as:

$$M(t_0) = E[M(t_0 | Z(t_0) = 1)] = E[M_{11} + M_{12} + \dots + M_{1n}] = \int_{t_0}^{\infty} \int_0^{\infty} \dots \int_0^{\infty} \left(\sum_{i=j}^n M_{ji}(t_0) \right) g_{x|x_j} dx_{n-1} \dots dx_j = \int_0^{\infty} M_{11}(t_0) g_1 dx_1 + \int_0^{\infty} \int_0^{\infty} M_{12}(t_0) g_1 g_2 dx_2 dx_1 + \int_0^{\infty} \int_0^{\infty} \dots \int_0^{\infty} M_{1n}(t_0) g_x dx_{n-1} \dots dx_2 dx_1 \tag{15}$$

2) An old component

For an old component, $T > t_0$ and $Z(\Delta_m) = j$. Whether the health condition $Z(t_0)$ is known to depend on whether t_0 is inspection point.

Situation S1: t_0 is exactly the inspection instant.

In this case, $t_0 = \Delta_m$ and $Z(t_0) = j$, MRL is denoted by:



$$\begin{aligned}
 M(t_0) &= E[M(t_0|Z(t_0) = 1)] = E[M_{j_1} + M_{j_2} + \dots + M_{j_n}] \\
 &= \int_{t_0}^{\infty} M_{j_1}(t_0)g_{j_1|x_1}dx_1 + \int_{t_0}^{\infty} \int_0^{\infty} M_{j_2}(t_0)g_{j_2|x_2}g_{j_1|x_1}dx_2dx_1 \\
 &\quad + \int_{t_0}^{\infty} \int_0^{\infty} \dots \int_0^{\infty} M_{j_n}(t_0)g_{j_n|x_n}dx_n \dots dx_2dx_1
 \end{aligned}
 \tag{16}$$

The old2 case: t_0 is between two successive inspection instants Δ_m and Δ_{m+1} .

Given t_0 and $Z(\Delta_m) = j$, MRL is calculated by:

$$M(t_0) = \sum_{i=j}^n \int_{Z(\Delta_m)=i} M(t_0|Z(t_0) = i)g_{x_i|x_j}dx_{n-1} \dots dx_{j+1}dx_j
 \tag{17}$$

The integral region of $m_i(t_0)$ is equal to:

$$\left\{ (X_1, X_2, \dots, X_j) \left| \begin{array}{l} x_j > \Delta_m - T_{j-1} \\ x_j + x_{j+1} + \dots + x_{i-1} < t_0 - T_{j-1} \\ x_j + x_{j+1} + \dots + x_i > t - T_{j-1} \end{array} \right. \right\}
 \tag{18}$$

Similar to the proof of (14), project the region onto the lower dimension space repeatedly so that the multiple integral is transformed into repeated integral. The upper and lower limits can be obtained as in (14).

The steps for evaluating SF and MRL are summarized as: ① obtain $t_0, \Delta_m, Z(\Delta_m), T_i, i < Z(\Delta_m)$ and determine $g_{x_i|x_j}$ according to historical inspection data; ② evaluate the survival function by (9), (11) and (13); ③ evaluate the mean residual life by (15), (16) and (17).

4 Numerical examples

The parameter estimation is not addressed in this paper. The DGA information and failure rate parameters in [24] are adopted. The first numerical example is to compare the results obtained by developed formulas with those of the Monte Carlo technique. In [25], the same reliability indices, SF and MRL, are evaluated by the Monte Carlo technique. The minimal errors indicate the accuracy of developed formulas.

Assume that the baseline function has a Weibull distribution and the link function follows exponential form:

$$\begin{cases} h_0(s) = \frac{\beta s^{\beta-1}}{\alpha^\beta} & s \geq 0, \alpha = 10, \beta = 2 \\ \psi(Z(s)) = e^{1 \times (Z(s)-1)} \end{cases}
 \tag{19}$$

For simplicity, we assume $n = 3$. In other words, the health condition is divided into 3 stages $\{1, 2, 3\}$ and the sojourn time X_1 and X_2 are s -independent and identically distributed Weibull random variables. The PDF of X_i is given:

$$g_i = g(x_i) = \frac{bx_i^{b-1}}{a^b} \exp \left[-\left(\frac{x_i}{a}\right)^b \right] \quad x_i > 0, i = 1, 2, \dots, n
 \tag{20}$$

where $a = 11.2838$ and $b = 2$. It is not hard to know $EX_i = 10$.

We sample X_1, X_2 by the Monte Carlo technique and calculate the SF and MRL by (6) and (8). The convergence condition is that the coefficient of variation is less than 0.05. For a new component $t_0 = 0, t = t_0 + 5$; for an old component, we presume $\Delta_m = t_0 = 4, Z(\Delta_m) = 1, t = t_0 + 5$ in case 1 and $\Delta_m = 4, t_0 = 5, Z(\Delta_m) = 1, t = t_0 + 1$ in case 2. The results given by the proposed analytical method and the Monte Carlo method are contrasted in Table 2 where old1 and old2 represent the two different cases for an old component, respectively.

From Table 2 we can see that the results obtained by the two methods are very close. Moreover, the proposed analytical formulas offer more advantages. Theoretically, the analytical formulas always provide a concise value which could be distinct from those offered Monte Carlo which varies based on the designated simulation parameters. The Monte Carlo method is based on the process of ‘‘sampling-evaluation-convergence’’ and the accuracy of results depends on the convergence condition and the number of samples. Although the uncertainty could be controlled within a given range, the evaluation results vary by samples. In other words, two sets of samples may pose different results even if they both satisfy the convergence conditions. On the other hand, the error in the proposed analytical method depends on rounding as long as the equations are stated correctly.

In the proposed model, the analytical method has a shorter calculation time and higher accuracy than the Monte Carlo method when $n \leq 4$. When n is larger than 5, the computation of repeated integral could be a heavy burden. Therefore the proposed analytical method no longer has a computation time advantage. However, the analytical formulas present a higher accuracy for either $n \leq 4$ or $n \geq 5$. In this numerical example, the calculation time

Table 2 SF and MRL given by RIBAM and Monte Carlo method

Calculation method	Survival function		Mean residual life			
	New	Old (S1)	Old (S2)	New	Old (S1)	Old (S2)
Analytical formulas	0.7511	0.4307	0.3666	7.6559	4.8342	4.3562
Monte Carlo	0.7535	0.4276	0.3704	7.7385	4.8870	4.2630

Table 3 SF and MRL given by analytical formulas and Monte Carlo method

Current time t_0	$\Delta = 0.4$			$\Delta = 0.8$		
	DMDT	CMCT	DMCT	DMDT	CMCT	DMCT
0	0.9984	0.9983	0.9983	0.9936	0.9935	0.9935
1	0.9904	0.9902	0.9901	0.9778	0.9767	0.9763
4	0.9670	0.9644	0.9644	0.9320	0.9222	0.9222
7	0.9440	0.9372	0.9310	0.8883	0.8644	0.8368
12	0.9070	0.8897	0.8897	0.8200	0.7677	0.7677
15	0.8855	0.8606	0.8398	0.7816	0.7116	0.6403
18	0.8645	0.8314	0.8314	0.7450	0.6581	0.6004
25	0.8174	0.7639	0.7234	0.6660	0.5449	0.5076
35	0.7456	0.6721	0.6453	0.5676	0.4126	0.3017
40	0.7250	0.6291	0.6291	0.5239	0.3583	0.3583
50	0.6692	0.5494	0.5494	0.4465	0.2698	0.1980

of SF is 0.18 s using the analytical method on a 2.6 GHz computer, while the time used by the Monte Carlo method varies between 0.5 s and 5 s.

In most practical cases, human operators would like to observe precise power transformer conditions. A large number of health condition stages will make the problem more complex and reduce the decision making efficiency. Moreover, the evaluation accuracy depends on the established model, monitoring data and parameters estimation. A large number of stages can reduce the evaluation efficiency and accuracy. Therefore, four stages of aging condition are deemed enough for the reliability evaluation of power transformers.

The DMDT models always assume that the equipment conditions stay the same between two successive inspection instances to make the SF calculation tractable. Furthermore, the CMCT model assumes rather superficially that the equipment condition would always be available. Hence, both models can produce errors. To illustrate the advantages of the proposed model, we concentrate on the equipment reliability in a single inspection interval. The survival function $P(T > t_0 + \Delta | T > t_0, Z(t_0) = 1)$ under $\Delta = 0.4$ and $\Delta = 0.8$ are shown in Table 3 and Figs. 3–5.

From Table 3, Figs. 3 and 4, we can see that the SF obtained from DMDT is always larger than that from DMCT, which means that we will overestimate the reliability if we ignore the state transition between inspection points. At the inspection points the results obtained by the CMCT and DMCT models are the same which are shown in bold in Table 3. The difference between DMCT and CMCT models is that DMCT model is under discrete monitoring while CMCT model is under continuous monitoring. However, at inspection points the state is known

and the uncertainty of $Z(t_0)$ is eliminated. Thus the difference between DMCT and CMCT disappears and the DMCT model degrades into the CMCT model.

For non-inspection points, the SF calculated in the DMCT model is smaller than that calculated in the CMCT model which is due to the possible state transition between the last inspection instant and the current time. The

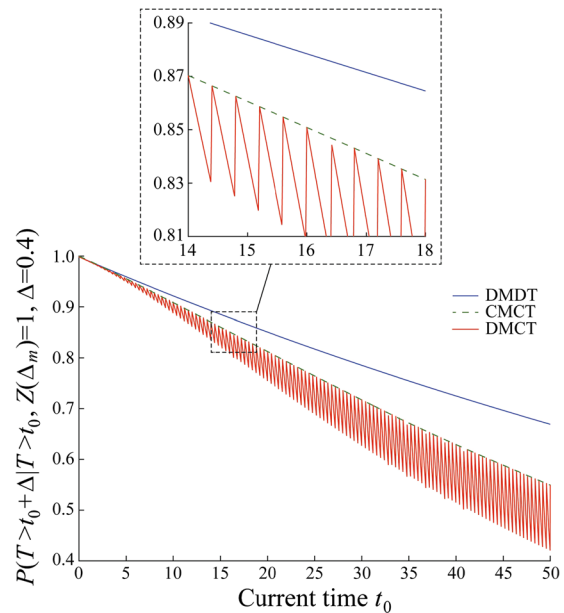


Fig. 3 Survival function when $\Delta = 0.4$

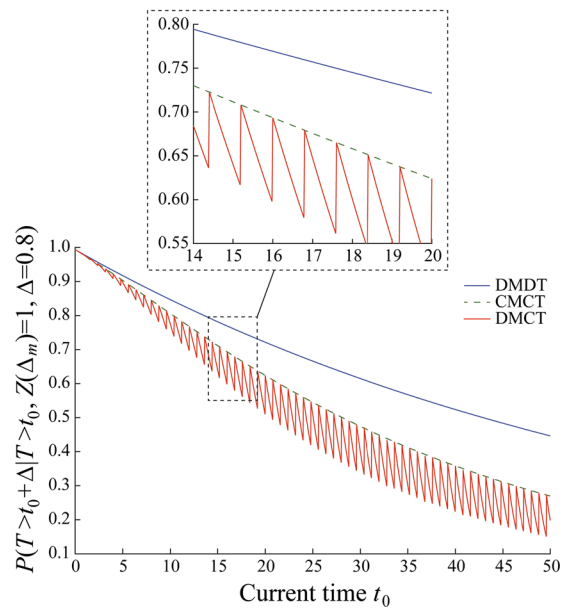


Fig. 4 Survival function when $\Delta = 0.8$



component reliability decreases with time in the long run. Besides, the DMCT curve shows that the reliability decreases deeper when $t_0 - \Delta_m$ is larger. It is reasonable to assume that the longer the difference between the last inspection instant Δ_m and the current time t_0 , the bigger would be the error if we regard $Z(t_0)$ as $Z(\Delta_m)$. Besides, the older component tends to pose a larger error. This confirms the intuitive notion that the longer a component stays in a state (except absorbing state), the higher is the likelihood that it would transit to another (mostly worse) state and the larger would be the error unless we consider the state transition within the next inspection interval.

Figure 5 shows how the health condition strongly affects the shape of SFs. The component condition transits from state 1 to state 2 at time 10. The worse health condition offers a sharper decrease in SF. The diversity of component health condition is not considered in the traditional exponential or the Weibull distribution which will lead to serious errors.

To illustrate the influence of Weibull parameters of sojourn time distribution (STD), we vary the shape parameter b from 0.5 to 5 and change the scale parameter a to make sure the expectation of sojourn time is 10. We include the coefficient of variation of the sojourn time distribution in Table 4 to gain more insight. CV is usually introduced to describe the dispersion degree of distribution. In this case, we would like to observe how the distribution

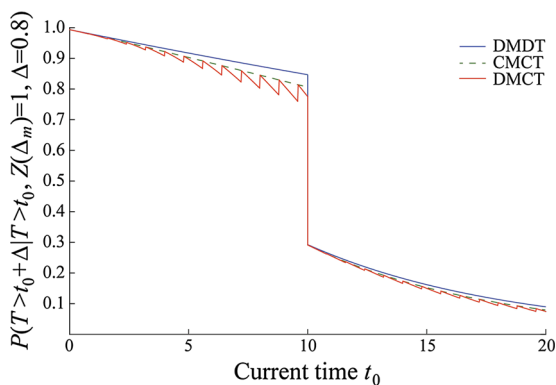


Fig. 5 Survival function under state transition at time 10

Table 4 SF and MRL in different Weibull distribution parameters

Sojourn time distribution	Coefficient of variation	Survival function $P(T > 5)$	Mean residual life
(5, 0.5)	2.2361	0.5237	5.7442
(8.8261, 0.8)	1.2605	0.6395	6.6986
(10, 1)	1	0.6795	7.0205
(11.2838, 2)	0.5227	0.7511	7.6559
(10.8912, 5)	0.2290	0.7768	7.9682

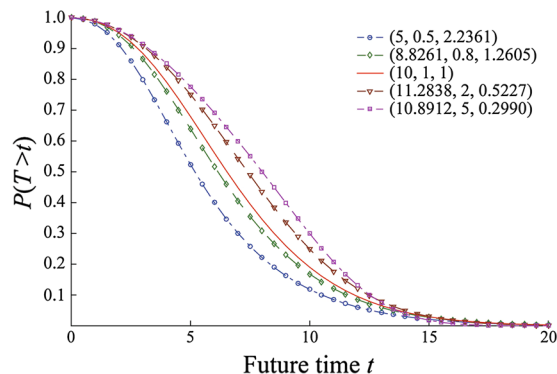


Fig. 6 SF under different Weibull sojourn time distribution

of condition sojourn time changes the reliability indices even though two distribution functions have the same expected condition sojourn time.

Five groups of parameters (a, b, CV) are $(5, 0.5, 2.2361)$, $(8.8261, 0.8, 1.2605)$, $(8.8261, 0.8, 1.2605)$, $(10, 1, 1)$, $(11.2838, 2, 0.5227)$, $(10.8912, 5, 0.2290)$. In Table 4, even though the five groups of transformers have the same expected condition sojourn time, they have different reliability indices. A bigger CV always leads to a lower survival function and shorter mean residual life.

The survival functions are calculated for a new component. The five SFs are shown in Fig. 6. The semi-Markov process degenerates to a Markov process when $b=1$. This observation implies that the error is inevitable if we always assume the state transition conforms to a Markov process. Another notable observation is that the variation in sojourn time distribution parameters can lead to a different SF curves, though they all follow the Weibull distribution and have the same mean value. The equipment reliability declines sharper with the increase in CV. It is reasonable to assume that a larger variability always offers a lower reliability and boosts the cost on maintenance. The MRLs shown in the last column in Table 4 indicates that larger CV also means a shorter mean equipment life. The presented results are for $n = 4$. There are similar conclusions for $n > 4$.

5 Conclusion

We develop analytical formulas based on a more realistic DMCT model for evaluating the equipment reliability of deteriorating systems. The DMCT model assumption ensures that the results agree with the practice. The minimal errors between analytical formulas and Monte Carlo results imply the accuracy of the proposed method. Furthermore, the proposed method offers more realistic results in a shorter calculation time.

By comparing SF and MRL in the three models, we learn that the reliability will be overestimated if we apply a DMDT model between inspection points. That is, assuming $Z(t_0) = Z(\Delta_m)$ or $Z(t) = Z(t_0)$ will bring inevitable errors. The longer inspection interval will result in a longer transition between the last and the current states with a larger error. For non-monitoring points, the DMCT results are different from those of CMCT. However, for the monitoring point, DMCT and CMCT models have the same results, i.e., the DMCT model degrades into the CMCT model. This also indicates that the CMCT model cannot conform to practical cases since it is unrealistic to obtain the health condition at all points. Another observation is that a larger CV always refers to a lower reliability despite the same state sojourn time expectation. We draw a conclusion that two sets of products will offer different reliability results although they have the same s -expected state sojourn time. Steady quality (means a smaller CV) is essential to achieve a higher reliability. A greater variation of quality always tends to shorten the MRL and boost the cost.

Open Access This article is distributed under the terms of the Creative Commons Attribution 4.0 International License (<http://creativecommons.org/licenses/by/4.0/>), which permits unrestricted use, distribution, and reproduction in any medium, provided you give appropriate credit to the original author(s) and the source, provide a link to the Creative Commons license, and indicate if changes were made.

Appendix A

Proof of (10)

To obtain (10) we need to transform the multiple integral r_{1k} into repeated integral which contains the following steps:

Step 1: determine the integral area.

In this case, the integral area is denoted by:

$$D_{1k} = \left\{ (X_1, X_2, \dots, X_k) \left| \begin{array}{l} x_1 + \dots + x_{k-1} \leq t \\ x_1 + \dots + x_k > t \end{array} \right. \right\} \quad s \leq k < n$$

$$D_{1n} = \{ (X_1, X_2, \dots, X_{n-1}) \mid x_1 + \dots + x_{n-1} \leq t \}$$

Step 2: project the integral area $D_{1k}(D_{1n})$ onto lower dimensional space.

In this step, we obtain projected area $d_{k-1} = \{X_1, \dots, X_{k-1} \mid x_1 + \dots + x_{k-1} < t\}$ and the integral $r_{1k} = \int_{d_{k-1}} \int_{t-x_1-\dots-x_{k-1}}^{\infty} R_{1k}(t) g_x dx_k \dots dx_2 dx_1$,
 $(r_{1n} = \int_{d_{n-2}} \int_0^{t-x_1-\dots-x_{n-1}} R_{1n}(t) g_x dx_{n-1} \dots dx_2 dx_1)$.

Step 3: Repeat step 2 and decrease the dimension of d_i in succession until the dimension of integral region projection is equal to 1, i.e. $i = 1$. Finally we can get (10).

Appendix B

Proof of (12)

The proof can be obtained as follows:

Step 1: determine the multiple integral area.

Since the state transition points have Markov property and the known condition is $Z(T_{j-1}) = j$, the integral region D_{jk} is:

$$\left\{ (X_j, X_{j+1}, \dots, X_k) \left| \begin{array}{l} x_j \geq t_0 - T_{j-1} \\ x_j + \dots + x_{k-1} < t - T_{j-1} \\ x_j + \dots + x_k > t - T_{j-1} \end{array} \right. \right\} \quad 1 \leq k < n$$

and D_{jn} is:

$$\left\{ (X_j, X_{j+1}, \dots, X_{n-1}) \left| \begin{array}{l} x_j \geq t_0 - T_{j-1} \\ x_j + \dots + x_{n-1} < t - T_{j-1} \end{array} \right. \right\}$$

Step 2: project the integral area D_{jk} onto lower-dimensional space (X_j, \dots, X_{k-1}) .

In this step, we obtain projected area $d_{j,k-1}$ is:

$$\left\{ (X_j, X_{j+1}, \dots, X_{k-1}) \left| \begin{array}{l} x_j \geq t_0 - T_{j-1} \\ x_j + \dots + x_{k-1} < t - T_{j-1} \end{array} \right. \right\}$$

and the integral is:

$$\int_{d_{j,k-1}} \int_{t-x_1-\dots-x_{k-1}}^{\infty} R_{jk}(t|t_0) g_{x|x_j} dx_k \dots dx_j.$$

For $k = n$, similar results can be obtained which will not be listed for simplicity.

Step 3: repeat step 2 and decrease the dimension of integral region projection in succession until the dimension equals 1.

We have $d_{j,j} = \{X_j \mid t_0 - T_{j-1} \leq x_j < t - T_{j-1}\}$ at last. Through steps 1 to 3 we get (12).

Appendix C

Proof of (14)

With $Z(\Delta_m = j)$, $Z(t_0) = i$, $Z(t) = k$, (15) can be obtained by following steps.

Step 1: the integral region $D_{j,ik}$ equals

$$\left\{ (X_j, X_{j+1}, \dots, X_k) \left| \begin{array}{l} \Delta_m < x_1 + \dots + x_j \\ x_1 + \dots + x_{i-1} < t_0 < x_1 + \dots + x_i \\ x_1 + \dots + x_{k-1} < t < x_1 + \dots + x_k \end{array} \right. \right\},$$

since the state transition points have Markov property and the known condition is $Z(T_{j-1}) = j$, the integral region D_{jk} is:



$$\left\{ (X_j, X_{j+1}, \dots, X_k) \left| \begin{array}{l} x_j \geq t_0 - T_{j-1} \\ x_j + \dots + x_{k-1} < t - T_{j-1} \\ x_j + \dots + x_k > t - T_{j-1} \end{array} \right. \right\}$$

for $1 \leq k < n$ and D_{jn} is:

$$\left\{ (X_j, X_{j+1}, \dots, X_{n-1}) \left| \begin{array}{l} x_j \geq t_0 - T_{j-1} \\ x_j + \dots + x_{n-1} < t - T_{j-1} \end{array} \right. \right\}$$

Step 2: project $D_{j,ik}$ on lower-dimensional space.

Step 3: repeat step 2 until the dimension of integral region is reduced to 1.

Denote the projection on space $\{X_j, \dots, X_h\}$ as v_h and then we get:

$$v_i = \left\{ (X_j, X_{j+1}, \dots, X_i) \left| \begin{array}{l} \Delta_m - T_{j-1} < x_j \\ x_j + \dots + x_{i-1} < t_0 - T_{j-1} \\ x_j + \dots + x_i > t_0 - T_{j-1} \\ x_j + \dots + x_i < t - T_{j-1} \end{array} \right. \right\}$$

$$v_j = \{X_j | \Delta_m - T_{j-1} < x_j < t_0 - T_{j-1}\}$$

Through step 1 to step 3 we can obtain (14) finally.

References

[1] Duval M (1989) Dissolved gas analysis: it can save your transformer. *IEEE Electr Insul Mag* 5(6):22–27

[2] Pham H (2006) *Handbook of engineering statistics*. Springer, New York

[3] Cao J, Cheng K (1986) *Introduction to reliability mathematics*. SciencePress, Beijing

[4] Bowles JB (2002) Commentary-caution: constant failure-rate models may be hazardous to your design. *IEEE Trans Reliab* 51(3):375–377

[5] Cox DR (1972) Regression models and life tables. *JR Stat Soc [b]* 34(2):187–220

[6] Farewell VT (1979) An application of Cox’s proportional hazard model to multiple infection data. *J R Stat Soc C-APP* 28(2):136–143

[7] Qiu J, Wang H, Lin D et al (2015) Nonparametric regression-based failure rate model for electric power equipment using lifecycle data. *IEEE Trans Smart Grid* 6(2):955–964

[8] Gasmi S, Love CE, Kahle W (2003) A general repair, proportional-hazards framework to model complex repairable systems. *IEEE Trans Reliab* 52(1):26–32

[9] Vlok PJ, Coetzee JL, Banjevic D et al (2002) Optimal component replacement decisions using vibration monitoring and the proportional hazards mode. *J Op Res Soc* 53(2):193–202

[10] Ji HX, Zhang JQ, Liu ZY et al (2010) Optimal maintenance decision of power transformers. In: *International conference on electrical and control engineering (ICECE)*, Wuhan, China, 25–27 June 2010, pp. 3941–3944

[11] Newby M (1994) Perspective on Weibull proportional-hazards models. *IEEE Trans Reliab* 43(2):217–223

[12] Banjevic D, Jardine AKS (2006) Calculation of reliability function and remaining useful life for a Markov failure time process. *IMA J Manag Math* 17(2):115–130

[13] Makis V, Jardine AKS (1991) Computation of optimal policies in replacement models. *IMA J Manag Math* 3(3):169–175

[14] Ghasemi A, Yacout S, Ouali MS (2010) Evaluating the reliability function and the mean residual life for equipment with unobservable states. *IEEE Trans Reliab* 59(1):45–54

[15] Ghasemi A, Yacout S, Ouali MS (2007) Optimal inspection period and replacement policy for CBM with imperfect information using PHM. *World Congr Eng Comput Sci* 247:247–266

[16] Ghasemi A, Yacout S, Ouali MS (2010) Parameter estimation methods for condition-based maintenance with indirect observations. *IEEE Trans Reliab* 59(2):426–439

[17] Banjevic D, Jardine AKS, Makis V et al (2001) A control-limit policy and software for condition-based maintenance optimization. *INFOR-OTTAWA* 9(1):32–50

[18] Wu X, Ryan SM (2011) Optimal replacement in the proportional hazards model with semi-Markovian covariate process and continuous monitoring. *IEEE Trans Reliab* 60(3):580–589

[19] Liu X, Li J, Al-Khalifa KN et al (2013) Condition-based maintenance for continuously monitored degrading systems with multiple failure modes. *IIE Trans* 45(4):422–435

[20] Cui M, Ke D, Sun Y et al (2015) Wind power ramp event forecasting using a stochastic scenario generation method. *IEEE Trans Sustain Energy* 6(2):422–433

[21] Cui M, Feng C, Wang Z et al (2017) Statistical representation of wind power ramps using a generalized Gaussian mixture model. *IEEE Trans Sustain Energy*. doi:10.1109/TSTE.2017.2727321

[22] Bi J, Lu M, Yang X et al (2014) A transformer failure rate model concerning aging process and equipment inspection data. In: *International conference on power system technology, Chengdu, China, 20–22 Oct 2014*, pp. 1363–1367

[23] IEEE Std C57.104-2008 (2009) IEEE guide for the interpretation of gases generated in oil-immersed transformers. IEEE Power & Energy Society

[24] Lu MM, Wang YF, Guo CX et al (2014) Failure rate model for oil-immersed transformer based on PHM concerning aging process and equipment inspection information. *Power Syst Prot Control* 42(18):66–71

[25] Wang YF, Bao YK, Zhang H et al (2014) Evaluating equipment reliability function and mean residual life based on proportional hazard model and semi-Markov process. In: *Proceedings of international conference on power system technology (POWERCON), Chengdu, China, 20–22 Oct 2014*, pp. 1293–1299

Yifei WANG received the Ph.D of Electrical Engineering at Zhejiang University in 2016. Currently he is an assistant professor of the school of Automation at Guangdong University of Technology, Guangzhou, China. His research area is reliability engineering, power system resilience and operation optimization.

Mohammad SHAHIDEPOUR is the Bodine Distinguished Professor and Chair in the Electrical and Computer Engineering Department at Illinois Institute of Technology (IIT), Chicago. He is the author of 300 technical papers and four books on electric power systems planning, operation, and control. He is the recipient of the 2004 IEEE Power System Operation Committee’s Best Paper Award, 2005 IEEE/PES Best Paper Award, 2006 and 2007 Outstanding Working Group Awards, the Edison Electric Institute’s Outstanding Faculty Award, HKN’s Outstanding Young Electrical Engineering Award, Sigma Xi’s Outstanding Researcher Award, IIT’s Outstanding

Faculty Award, and the University of Michigan's Outstanding Teaching Award. He is also a Research Professor at the King Abdulaziz University in Saudi Arabia.

Chuangxin GUO received the B.Sc., M.Sc. and Ph.D degrees in Electrical Engineering from Huazhong University of Science and

Technology, Wuhan, China, in 1992, 1994 and 1997, respectively. From 1997 to 2003, he worked as the Director of Beijing Dongfang Electronics Research Institute and the Deputy Chief Engineer of Dongfang Electronics Co., Ltd. Since September 2006, he has been the professor in College of Electrical Engineering (CEE), ZJU. He is also the vice dean of CEE, ZJU.

